Alexander Kirshen, David Boutt, Daniel Corkran, Brendan Moran, & Rachel King

Executive Summary

We present the results of our 2 year study investigating the current status of saltwater intrusion into the Plymouth, Massachusetts region. We integrated existing information on water quality with newly created numerical models to assess the likelihood of saltwater intrusion under changing climatic conditions and sea-level rise scenarios. The new numerical models of groundwater flow and salt transport were developed based on the existing groundwater flow model of the region. We incorporated the physics of how salt and fresh interact and mix together with the latest projections of sea-level rise in the Cape Cod Bay region. The analysis of the current state (2023) of saltwater intrusion shows limited increases in subsurface salinity (salt water) in the aquifer along the coast that is localized in a few specific regions. At the larger aquifer scale the sources of salinity to the aquifer are localized to specific land uses (road salting and septic return flows) that are the current dominant source of salinity to the aquifer.

The forward looking simulations of saltwater intrusion due to sea-level rise, water use increase, and terrestrial climate changes show limited onshore movement of saltwater. We map out three potential areas of the largest changes. These are in areas of low topography and show 600 feet of lateral migration. Select regions experience up to 3-4 time increases in salinity associated with ~ 6

feet of sea-level rise. Based on the modeling results presented we have the following recommendations and suggestions:

- Encourage the town of Plymouth to develop a data dashboard to post salinity observations of town water supplies wells on an annual basis.
- Raise funds to perform an airborne electromagnetic geophysical survey of coastal areas to image the extent of saltwater intrusion (to test modeling) and document the hydrostratigraphic architecture of key coastal areas (See section 9.1.4)
- Develop an early warning system for subsurface salinity changes in key coastal areas (documented in Task 9.3.1)
- Develop and maintain a salinity database for surface and groundwaters across the town.
- Consider the suggested recommendations in section 9.3.2 for optimal placement of freshwater production wells.

Task 9.1 Predict and Identify Location of FW/SW interface (Final Maps and Report showing modeled position of current interface)

Model Domain

The 595 km^2 model domain was modified from Masterson et al. (2009) and contains portions of Marshfield, Pembroke, Duxbury, Kingston, Plympton, Plymouth, and Borne. The western boundary represents the groundwater divide and was delineated from the steady-state head distribution from Masterson et al. (2009), while the eastern boundary extends ~5 km offshore. The top of the model grid represents the ground surface and was developed by merging the MassGIS 1 meter Lidar DEM with Massachusetts Coastal Zone Bathymetry from Andrews et al. (2018). The bottom of the model grid represents 15 m below the top of bedrock. The bedrock surface was developed by merging a bedrock elevation map from Mabee et al. (2022) and a modified version of offshore bedrock elevation from Stone & Stone (2019). The model contains 18 layers with model cells 100 m wide and 100 m long. Cell thickness varies based on ground surface elevation and proximity to sea level. All mentioned elevations are in NAVD 88. Cell thicknesses are 4 m from 8 to -32 m asl, 8 m from -32 to -56 m asl, and 16 m from -56 to -120 m asl. The top elevation of cells representing the ground surface were set to the top of the model domain and range in thickness from 0.1 to 116 m.

Boundary Conditions

A three-dimensional, numerical, control-volume finite difference variable-density groundwater flow and transport model was developed in MODFLOW 6 (Langevin et al., 2023). Boundary conditions were assigned to the model to represent environmental and anthropogenic forcings. The constant head (CHD) boundary represents the ocean head and is assigned to cells with cell top elevations less than 0 m asl along the top of the model. Baseline sea level is the mean hourly sea level from April 2022 to April 2023 from NOAA Boston, Ma site (0.052 m asl). Recharge with a TDS of 100 mg/l enters the top of the model except for in the ocean (CHD cells). Recharge (RCH)

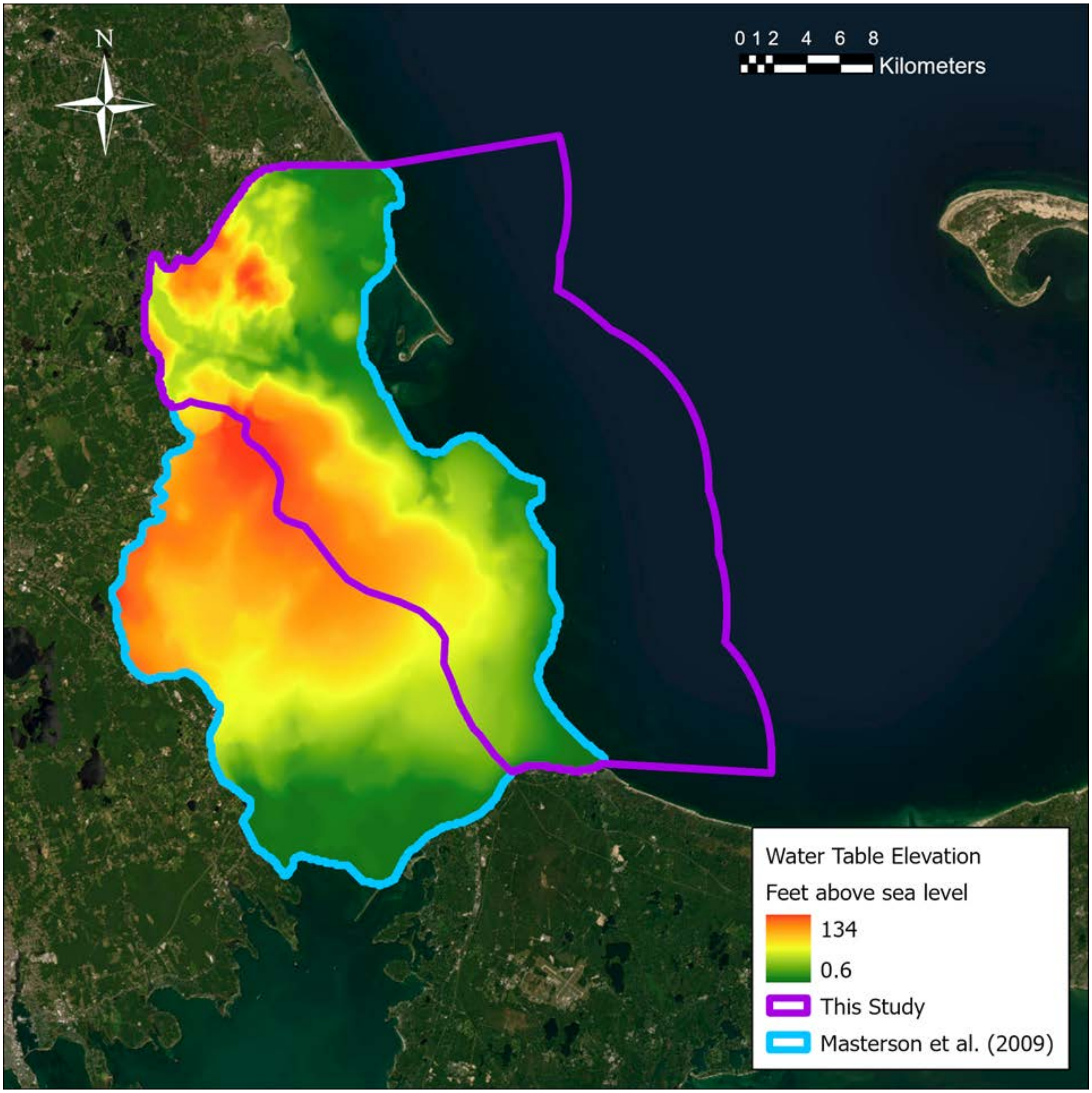

Figure 9.1-1: Model domain and steady-state hydraulic head from Masterson et al. (2009) and the modified model domain from this study.

varies for glacial aquifer sediments (0.0019 m/day), ponds (0.0014 m/day), wetlands (0.0005 m/day), and cranberry bogs (0.0007 m/day) (Masterson et al., 2009). The river package (RIV) is used for cells containing streams and rivers. Conductance for the rivers was calculated using a vertical hydraulic conductivity of 6.1 m/day, stream width of 3 m, and variable stream length based on the length of the stream within each cell (Masterson et al., 2009). Ponds, lakes, and reservoirs with an area greater than 8,000 m^2 (186 total) were modeled as high hydraulic conductivity zones with values ranging from 1,332 to 15,240 m/day. Pond hydraulic conductivities were calculated as the ratio of pond depth to cell thickness multiplied by 15,240 m/day (or 50,000 ft/day) (Masterson et al., 2009).

Anthropogenic forcings consist of pumping wells (WEL package), centralized wastewater re-infiltration (WEL package), and septic system return flow (RCH package). Public water supply wells and centralized wastewater re-infiltration sites are from the 2030 Masterson et al. (2009) model, and septic system return flow locations are assigned to cells containing waterlines but no sewer lines (Masterson et al., 2009). Along the eastern margin of the model, a constant concentration (CNC) boundary with TDS of 35,000 mg/l represents ocean salinity.

Baseline well pumping values were calculated using data from the 2019 Plymouth Draft Water System Master Plan Report. Pumping locations, elevations, and discharge were extracted from the 2030 Masterson et al. (2009) model. Total discharge in Plymouth for the year 2023 from the projected water demand forecast in the Draft Report was compared to discharge from the corresponding wells from Masterson et al. (2009). The 2023 Draft Report values comprise 77% of discharge from the 2030 model values. To calculate initial pumping for this model, all 2030 Masterson et al. (2009) production, commercial, and centralized re-infiltration discharge was multiplied by this factor of 0.77. Irrigation well pumping was not changed because irrigation was not predicted to have relevant increases between 2005 and 2030 (Masterson et al., 2009). Septic system return flows were divided into 6 zones based on Masterson et al. (2009) – Plymouth, North Sagamore, Duxbury, Marshfield, Pembroke, and Kingston. We assume that 85% of commercial and production well pumping is re-infiltrated via centralized wastewater return flow (onshore and offshore) and septic system return flow. Starting pumping values for irrigation already account for a 50% re-infiltration rate (Masterson et al., 2009).

Calibration

The groundwater flow models were calibrated with 36 groundwater and 36 surface water observation points (72 total) from Table 1-6 in Masterson et al. (2009) report. Hydraulic conductivity was modified manually to match simulated heads to observed heads. The root mean squared error (RMSE) and mean absolute error (MAE) for the model are 2.0 m (5.5%) and 1.4 m (3.8%), respectively.

Task 9.1.1 & 9.1.2 Assess location of current modeled FW/SW mixing zone (2023) & Produce detailed maps of modern salinity distribution

Simulated salinity for the year 2023 represented as total dissolved solids (TDS) ranges from 90 to 35,000 mg/l (Figure 9.1.1-1). While the majority of the model cells have concentrations of 0-100 and 10,000-35,000 mg/l, the freshwater/saltwater mixing zone is represented by the 1,000-10,000 mg/l zone (yellow). In general, this zone begins where the land surface meets the ocean and is 100 to 200 meters wide at the water table. Elevated TDS concentrations of 100-1,000 mg/l (green) extend 100 to 4,000 m landward.

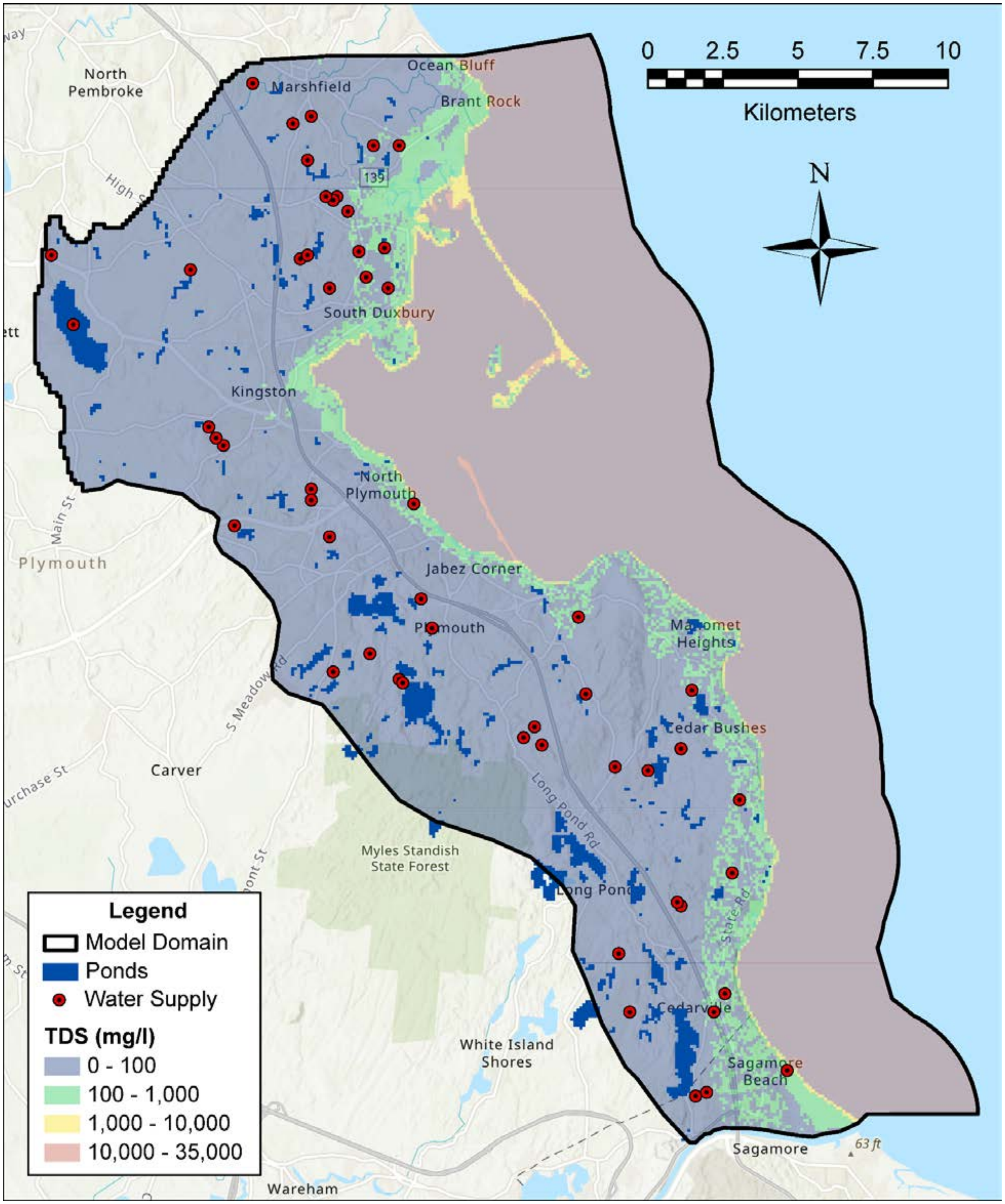

Figure 9.1.1-1: Simulated modern salinity distribution (TDS) in 2023 with locations of modeled water withdrawals and ponds.

Task 9.1.3 Determine relationship between pond geographical position and geometry and FW/SW mixing zone

Three ponds have TDS concentrations above 100 mg/l: Allens Pond, Scokes Pond, and Center Hill Pond. The relationship between pond geometry and the freshwater-saltwater mixing zone is shown in Figure 9.1.3-2, and the location of these cross-sections are in Figure 9.1.3-1. The mixing zone (1,000-10,000 mg/l) is represented by the light blue and light green colors. The distance between the mixing zone and Allens Pond, Scokes Pond, and Center Hill Pond are 100, 200, and 0 m, respectively.

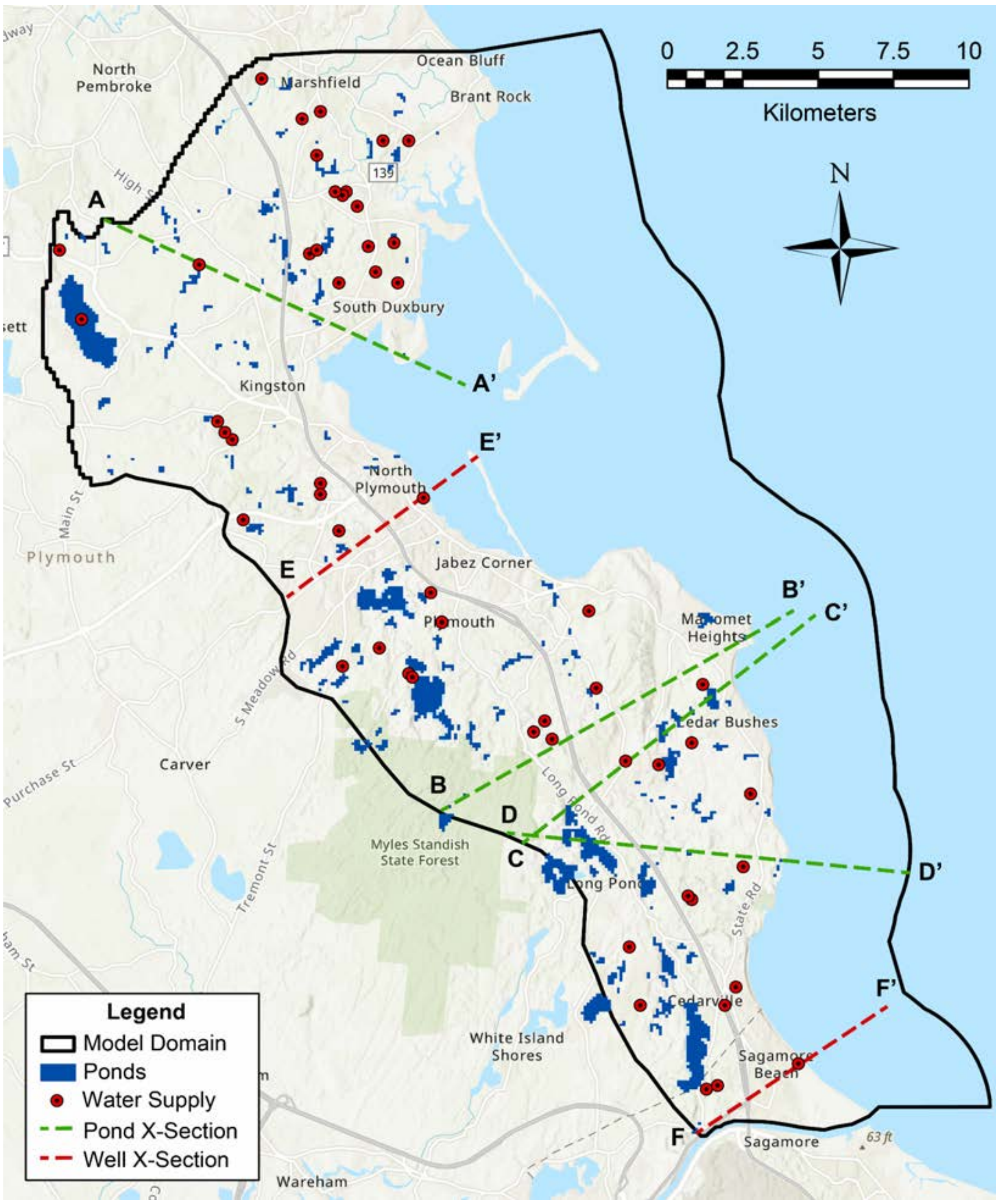

Figure 9.1.3-1: Lines showing cross-sections in Figures 9.1.3-2 and 9.2.2-2.

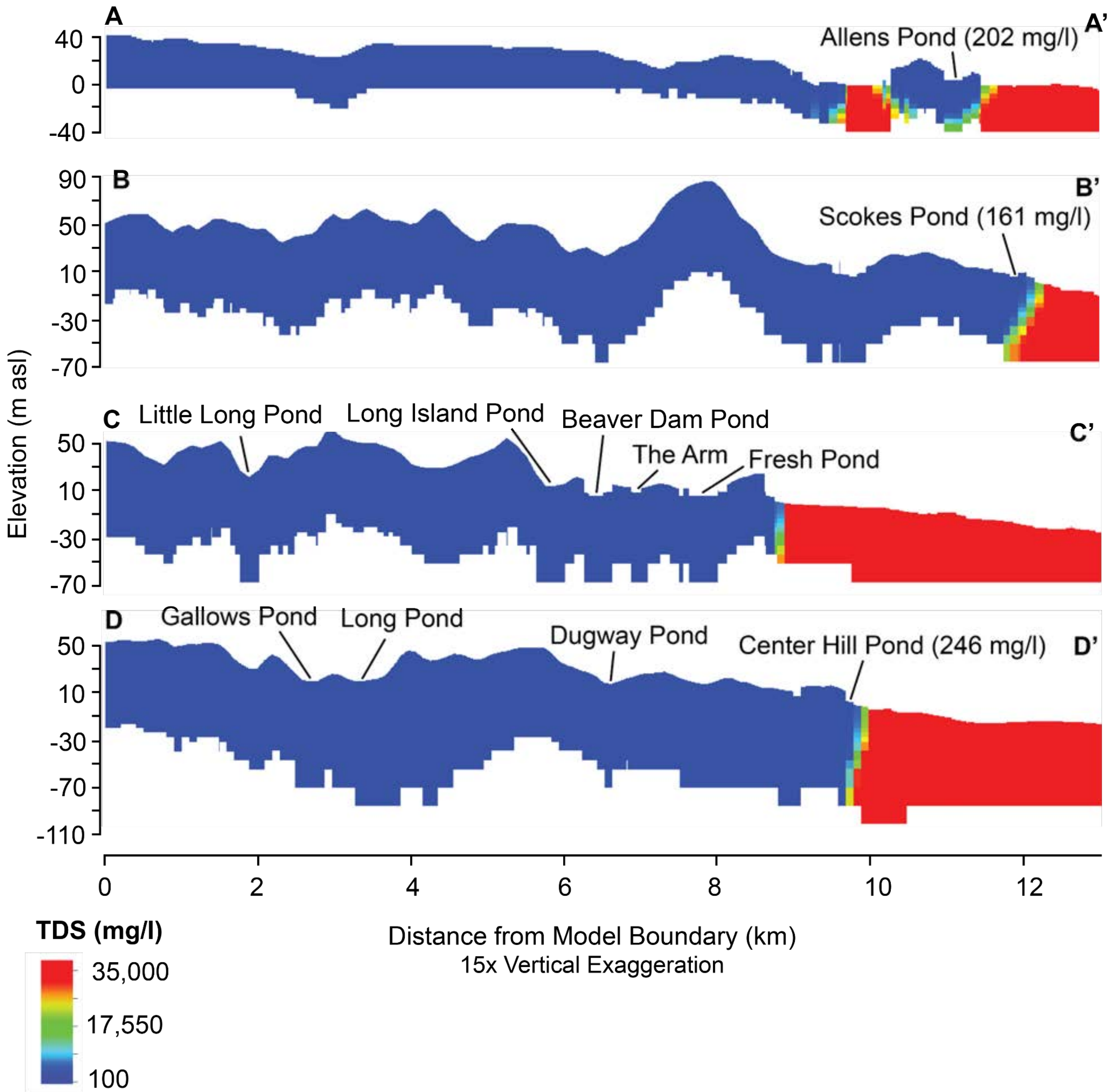

Figure 9.1.3-2: Cross-sections through coastal ponds (labeled) showing the top and bottom model boundaries and modern salinity distributions (color). All ponds have TDS concentrations of 100 mg/l if not otherwise labeled.

Task 9.1.4 Make recommendations using model select a few locations to perform geophysical investigations of interface geometry

Based on the groundwater flow model there are areas that experience higher probability of saltwater intrusion and are more likely to be impacted. The study found that high levels of saltwater intrusion are limited to the areas close to the coast. Geophysical surveys are necessary to further quantify the risks coastal communities may be facing. Current knowledge of subsurface materials is limited and was examined using drillers well logs throughout the project (Figure 9.1.4-1). Well logs are useful in characterizing grain size and soils. However, in order to create a more cohesive dataset that can be applied to climate resilience strategies, it would be beneficial to run an Airborne Electromagnetic Survey (AEM). This type of survey is performed by an instrument that is attached to a helicopter and flown across specific flight lines. The instrument transmits and receives electromagnetic waves, the response from the subsurface due to these waves is then measured to determine the conductivity of the materials. Using general conductivities, for example salt water is very conductive, salt water is more conductive than freshwater, bedrock is not very conductive, interpretation can be made to locate coastal confining units that would affect saltwater intrusion and general groundwater flow.hanse

The survey would run from about 500 meters onshore to 2 km offshore. Initial subsurface investigations into the Plymouth-Carver-Duxbury-Kingston aquifer system showed there are coastal silts clays that existed roughly seven meters onshore and into Plymouth Harbor (Hansen & Lapham, 1992). The location of where the Plymouth Carver sand and gravel aquifer extends offshore is not well characterized. Using AEM techniques, lithologies can be identified and the aquifer can be further mapped. In Monterey Bay, California, saltwater intrusion was mapped 3.5km offshore and up to 18m depth. The survey was able to penetrate through the conductive sea water and observe the underlying marine sediments. The saltwater-freshwater interface was identified because AEM data was able to show the water quality in offshore aquifers (Goebel et al., 2019).

Based on our existing findings, an AEM survey is a logical next step. Interpretation of AEM data requires ground truthing from well logs, surficial geology, and known water salinity. As part of the current project there is a comprehensive salinity database that shows areas of confirmed high conductivity conditions. Flight lines can be designed to investigate wells with elevated salinities and target areas that are most susceptible to saltwater intrusion (noted in pink in Figure 9.1.4-1). Based on available data, the southern region near Ellisville would be most beneficial for an AEM survey.

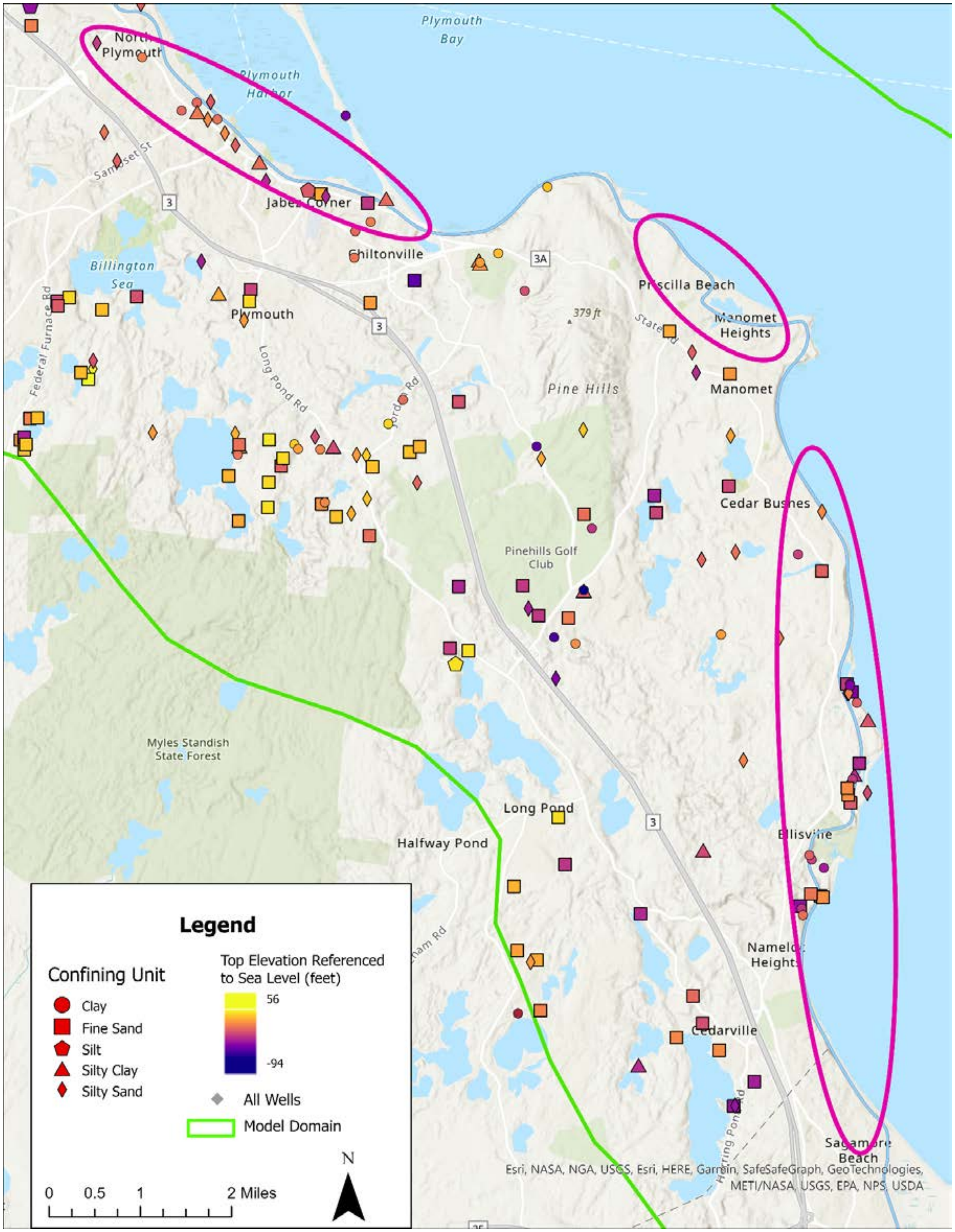

Figure 9.1.4-1: Map of wells that have a confining unit described in drillers logs (shape) and the associated top elevation of the unit (color). Key areas for geophysical investigation are shown as purple polygons.

Task 9.2 Assess (future looking) Different Mechanisms of Saline Intrusion and Vulnerability to Freshwater Aquifer System and Flow Paths

Task 9.2.1 Define Scenario-based modeling using stakeholder input

We developed a set of sea level and hydroclimate scenarios based on the latest climate change projections designed to predict changes to groundwater levels and salinity in the Plymouth aquifers through 2100. Monthly time series of two sea level scenarios representing the high and low potential rise and a wetter and dryer potential outcome based on high emissions scenarios were used to drive coastal and land surface recharge boundary conditions.

Table 1 summarizes the predicted sea level rise under these two scenarios. Monthly times series were developed by interpolating between decadal predictions through 2100 provided by Douglas and Kirshen (2022). We used these two scenarios to bound the potential for sea level change outcomes with a low-end, optimistic emissions scenario (RCP 2.6) and corresponding sea level rise of about 43 cm by 2100, and the highest sea level rise scenario which includes major Antarctic ice sheet loss and about 180 cm of sea level rise. We believe the results of these two scenarios allow us to assess the potential of the full range of likely outcomes at the Plymouth coast and in its aquifers.

Table 1: Modeled sea level rise scenarios through 2100 showing the increase in sea level relative to the 2020 baseline.

Scenario	**2040**	**2060**	**2080**	**2100**
Low-End RCP 2.6 Emissions	12.5 cm	24.5 cm	34.3 cm	43.0 cm
High-End (Major Antarctic ice sheet loss)	21.8 cm	57.9 cm	111.9 cm	180.5 cm

There is a substantial amount of uncertainty that remains in global climate projections regarding the predicted changes in precipitation patterns likely over the coming decades. Most of them predict our region will become wetter overall but the magnitude and seasonality of this change still have a large range of potential outcomes. The highest emissions scenario modeled by global climate simulations has a large magnitude of change and also larger ranges of possible precipitation patterns and magnitude changes. These scenarios include the wettest overall outcome for our region and also the driest overall, although still predict a slight increase in annual precipitation. The changes in the drier scenario are primarily reflected in large decreases in Summer and Fall precipitation which can have major impacts on the groundwater hydrology of the region.

We took a similar approach to sea level in developing time series' of the expected change in hydroclimate over the model domain through 2100 by modeling the highest emission projections and the corresponding wet (90th percentile probability) and dry (10th percentile probability) range in precipitation changes. This is intended to bound our model simulation results by depicting two plausible but highest-impact outcomes on the hydrology of the model region. Changes in precipitation are applied to the four recharge zones in our model by modulating the baseline monthly recharge rates through those zones. Monthly time series' of these change factors through 2100 were developed based on ranges in decadal precipitation changes under different emissions scenarios from Douglas and Kirshen (2022). The seasonal precipitation changes from which these time series were developed are summarized in Table 2.

Table 2: Modeled precipitation changes scenarios (reflected as recharge in the model) through 2100 showing the percentage change in precipitation relative to the 2020 baseline.

RCP 8.5 Emissions wet end-member	**2040**	**2060**	**2080**	**2100**
Winter (DJF)	+12.6 %	+24.7%	+34.8%	+44.8%
Spring (MAM)	+10.8%	+20.0%	+23.9%	+27.9%
Summer (JJA)	+8.2%	+14.5%	+15.6%	+16.7%
Fall (SON)	+7.5%	+13.5%	+14.9%	+16.3%
RCP 8.5 Emissions dry end-member	*2040*	*2060*	*2080*	*2100*
Winter (DJF)	+2.4 %	+4.5%	+5.5%	+6.4%
Spring (MAM)	+0%	+0.6%	+3.1%	+5.5%
Summer (JJA)	-3.3%	-7.5%	-14.5%	-21.6%
Fall (SON)	-3.8%	-7.4%	-10.7%	-14.0%

We developed a projected pumping scenario through 2100 based on the Draft 2019 Plymouth Master Water Plan Report and an informal discussion with an engineer from Environmental Partners - the consulting group leading the report (Figure 9.2.1-1). It is important to note that the projection beyond 2040 has not been evaluated by an engineer or planner. The Draft Report calculates future water demand in Plymouth through 2040 based on historic water use and projected population growth.

For the purpose of this study, we present the results from the high-end sea level rise and dry end-member recharge scenarios to investigate maximum saltwater intrusion in this region. For terrestrial recharge, we did not use a specific scenario, but an overall 15% reduction in recharge from baseline values. The four simulations presented in this document are in Table 3.

Table 3: Simulations and their respective flow model environmental and anthropogenic forcings.

Simulation	Flow Model Forcings
Simulation 1 (All Forcings)	Terrestrial recharge (baseline constant), well pumping (time-dependent), centralized wastewater re-infiltration (time-dependent), septic return flow (time-dependent), & high-end sea level rise (time-dependent)
Simulation 2 (No Septic Return Flow)	Terrestrial recharge (baseline constant), well pumping (time-dependent), centralized wastewater re-infiltration (time-dependent), & high-end sea level rise (time-dependent)
Simulation 3 (Only SLR & Recharge)	Terrestrial recharge (baseline constant) & high-end sea level rise (time-dependent)
Simulation 4 (All Forcings - 15% Recharge Reduction)	Terrestrial recharge - 15% reduction (constant), well pumping (time-dependent), centralized wastewater re-infiltration (time-dependent), septic return flow (time-dependent), & high-end sea level rise (time-dependent)

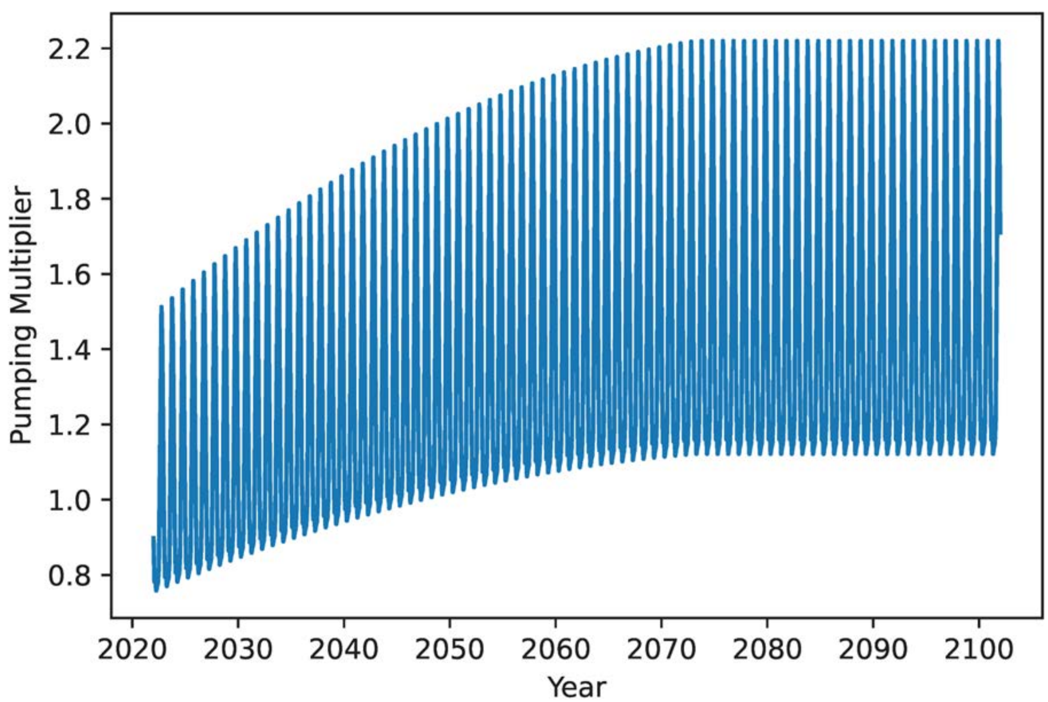

Figure 9.2.1-1: Projected water demand multiplier applied to all commercial and production wells, which includes seasonal variations in pumping.

Task 9.2.2 Determine Up-coning and lateral movement of interface due to on-shore freshwater production wells

Up-coning and lateral movement of the interface occurs at one well location within the model - DEP Well 4036002-02G. Figure 9.2.2-1 demonstrates how pumping causes increases in TDS in this well. Simulation 3 (green line) - no pumping or re-infiltration - has the lowest concentrations and smallest increase from 2020 to 2100 (112 mg/l), while Simulation 1 - all forcings - has larger concentrations and a larger increase from 2020 to 2100 (171 mg/l). The orange line - Simulation 2 with no septic system re-infiltration - has the largest concentrations and largest increase from 2020 to 2100 (330 mg/l), illustrating how septic system re-infiltration can buffer saltwater intrusion. The location and depth of this well in relation to mixing zone migration is shown in Figure 9.2.2-2. Well 4036002-02G (F-F') is 0 m from the freshwater-saltwater mixing zone, and model cells directly surrounding the well increased by 1 to 602 mg/l TDS from 2020 to 2100. The Plymouth Water Supply Well (E-E') is 200 m from the freshwater-saltwater mixing zone, and model cells directly surrounding the well increased by ~0 mg/l TDS from 2020 to 2100.

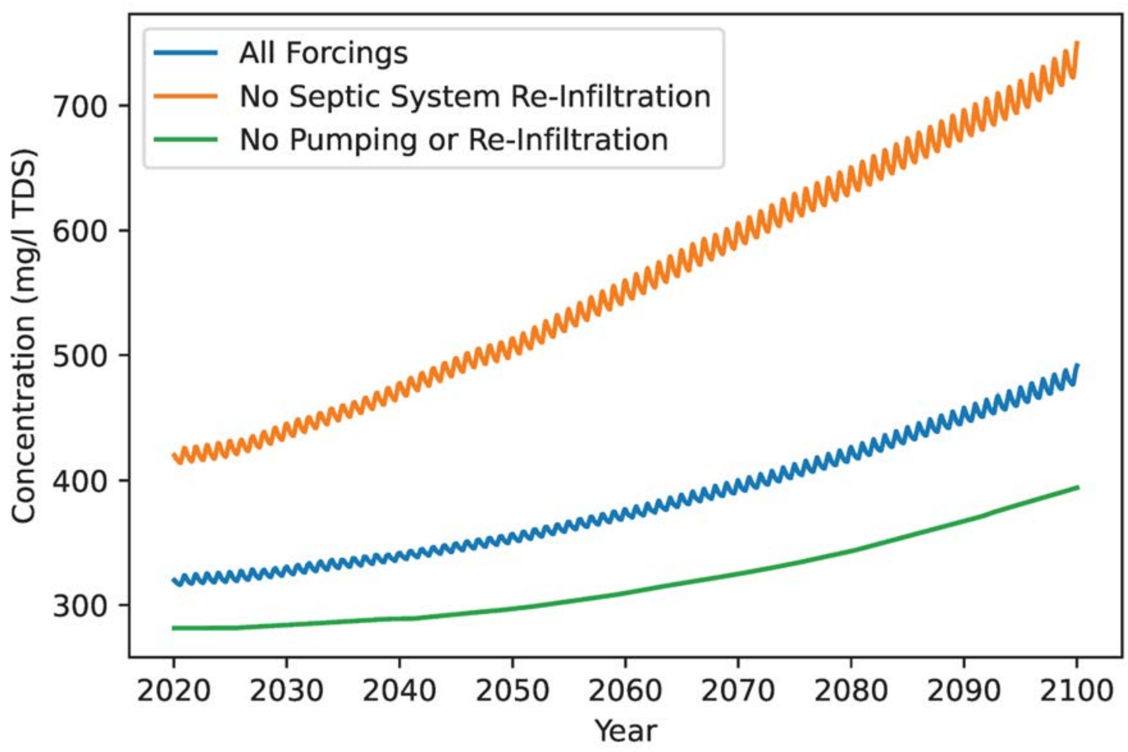

Figure 9.2.2-1: TDS concentrations from 2020 to 2100 being pumped from the bottom layer of the screened interval of DEP Well 4036002-02G (shown in Figure 9.2.2-2), which extends through 3 model layers.

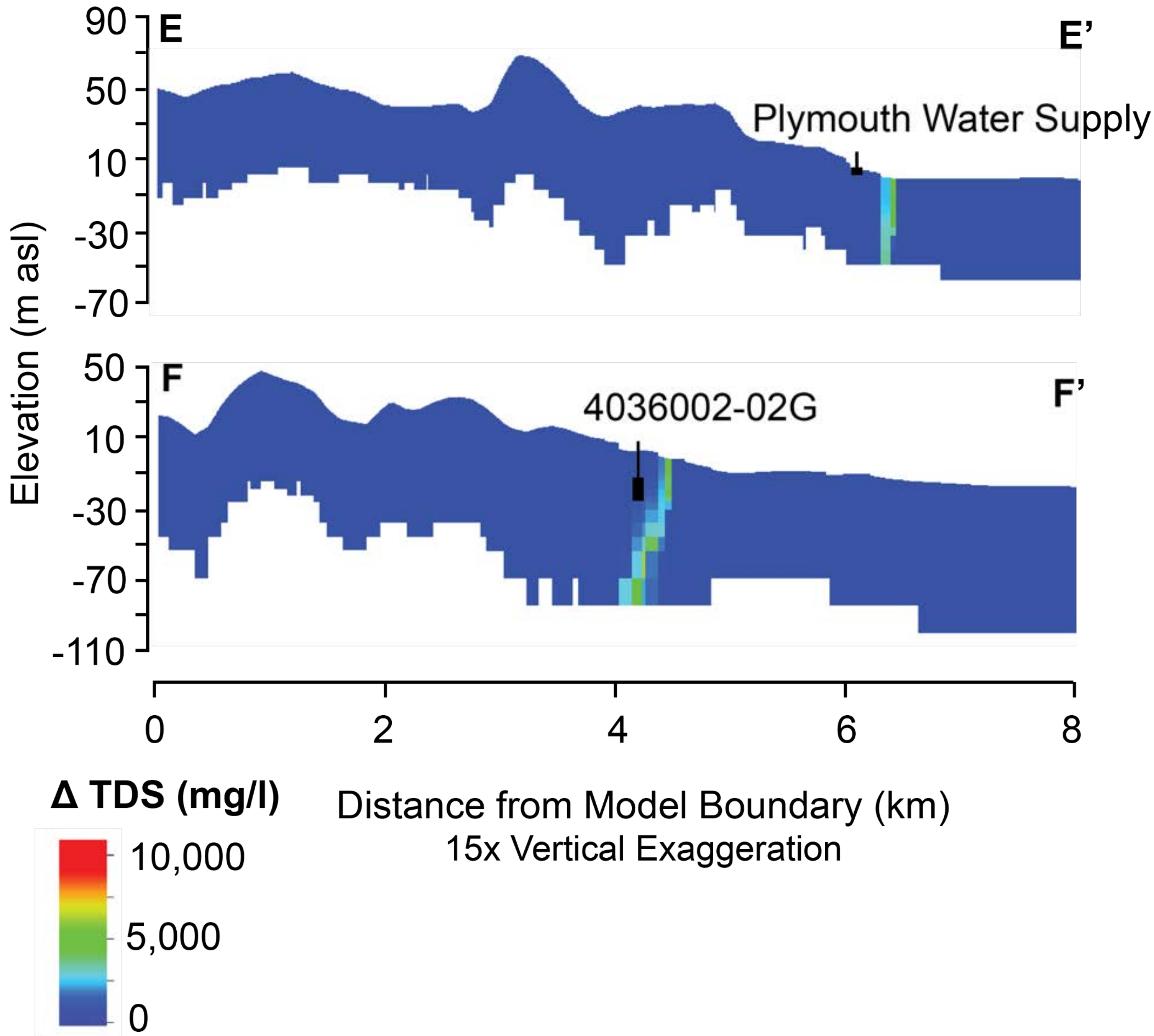

Figure 9.2.2-2: Cross-sections with the concentration increase from 2020 to 2100 (Δ TDS) in Simulation 1 . Well screen intervals are shown as black rectangles. Locations of the cross-sections are shown in Figure 9.1.3-1.

Task 9.2.3 Predict On-shore migration of interface mixing zone due to sea level rise (SLR)

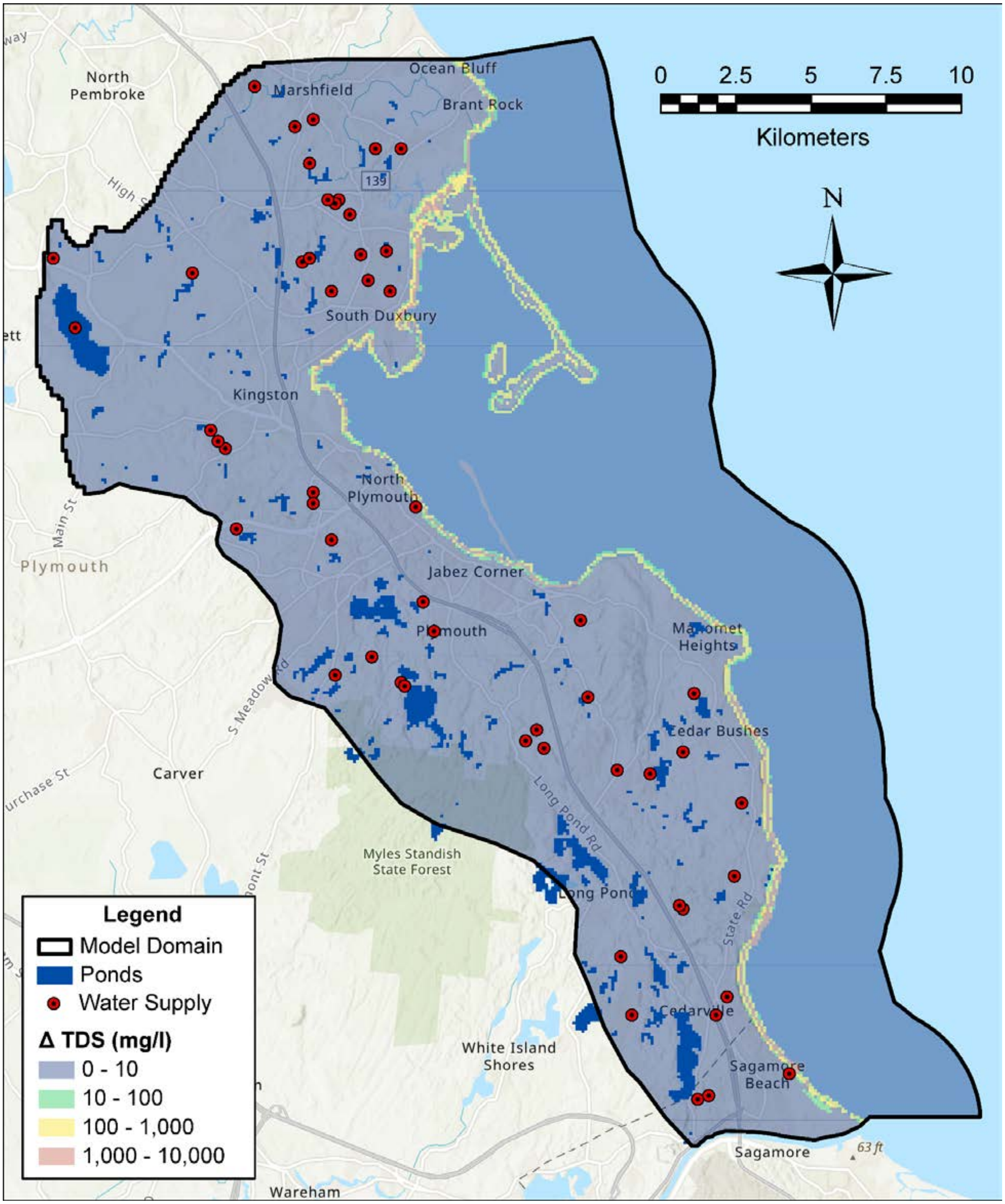

Figure 9.2.3-1: Concentration increase from 2020 to 2100 (Δ TDS) in Simulation 1 showing the landward migration of the interface mixing zone.

Changes in total dissolved solid concentrations from 2020 to 2100 in Simulation 1 range from 0 to 17,516 mg/l and are mainly driven by sea level rise (Figure 9.2.3-1). The zone representing TDS increases of 1,000-10,000 mg/l is generally 100 m wide at the water table but can extend to ~500 m wide in coastal marsh and estuary environments in the northern region of the model domain. Between Manomet Heights and Sagamore beach this zone increases in width to ~300 m below elevations of -28 m asl. This zone also increases in width to ~200 m between South Duxbury and Ocean Bluff between -16 and -32 m asl.

Task 9.2.4 Document possible re-modification of freshwater discharge patterns due to SLR

Coastal and stream discharge varies due to sea level rise throughout the model simulations. The total volume of water leaving the model through the RIV boundary increases by 6% between 2020 and 2100 (Figure 9.2.4-1). Rising sea levels cause water table elevations to increase leading to a larger hydraulic gradient between the RIV boundary and hydraulic heads, which increase discharge out of RIV boundary cells. The total water volume leaving the model through the CHD boundary decreases by 12% between 2020 and 2100 because as sea level rises, the hydraulic gradient between CHD boundary cells and the water table decreases (Figure 9.2.4-2).

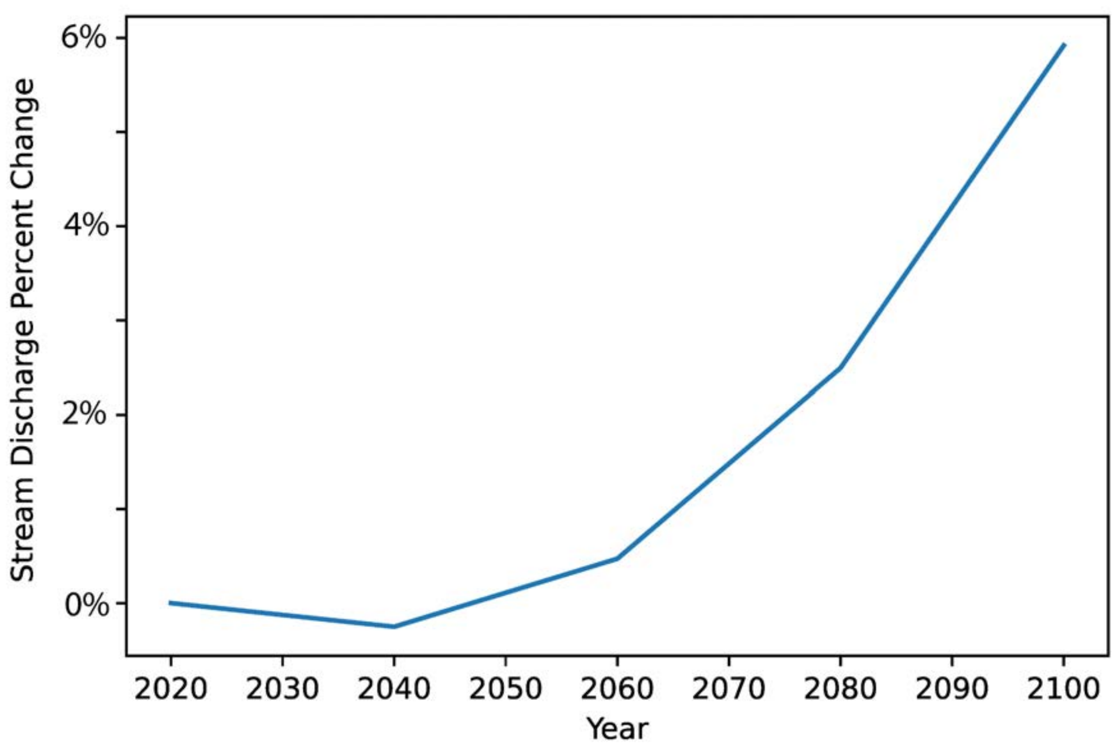

Figure 9.2.4-1: Percent change in total water volume leaving the model through the RIV boundary in Simulation 1 from 2020 to 2100 at 20-year intervals

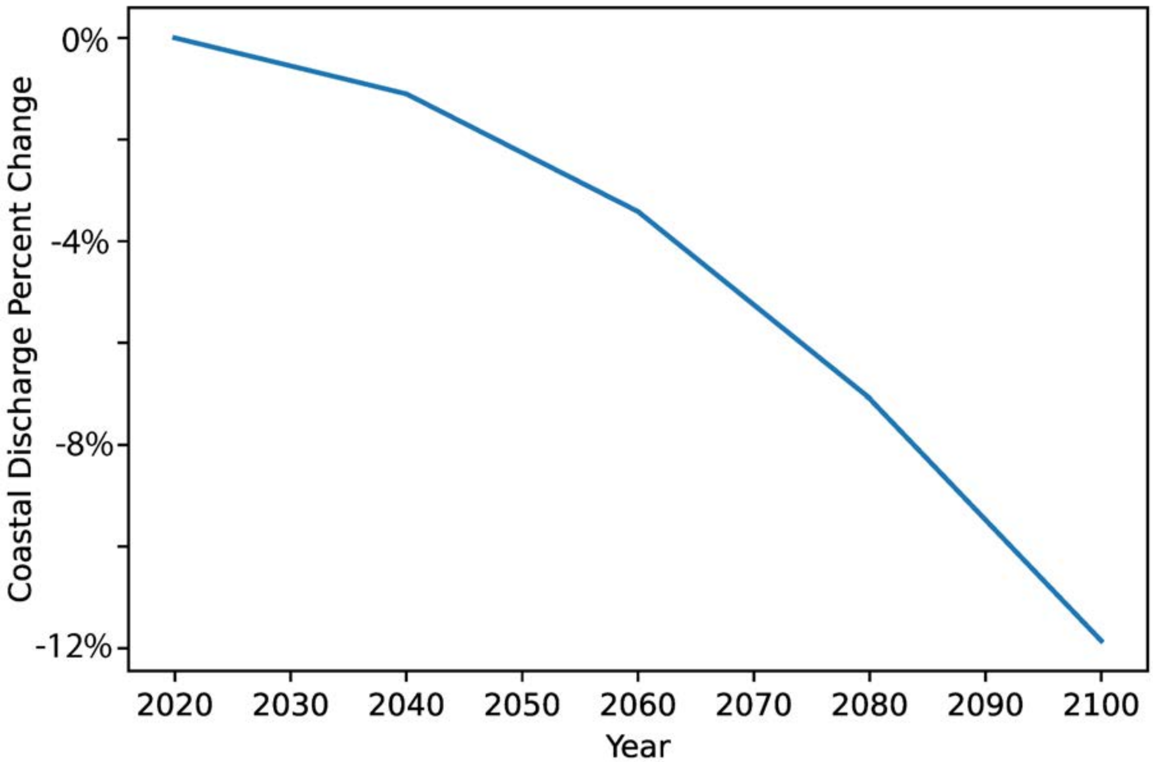

Figure 9.2.4-2: Percent change in total water volume leaving the model through the CHD boundary in Simulation 1 from 2020 to 2100 at 20-year intervals.

Task 9.2.5 Predict changes in salinity of near shore waters due to combined effects of SLR and pumping (water use)

Two ponds have increases in salinity in Simulations 1 and 2. In Simulation 2, which represents the largest possible concentration increase, the TDS of Allens Pond and Scokes Pond increase by 26 and 24 mg/l, respectively (Figure 9.2.5-1). In Simulation 1, TDS concentrations of these ponds only increase by 4 and 11 mg/l, respectively because septic system return flow buffers mixing zone migration. In both simulations, Center Hill Pond decreases in TDS concentration. The location of these ponds is shown in Figure 9.1.3-2.

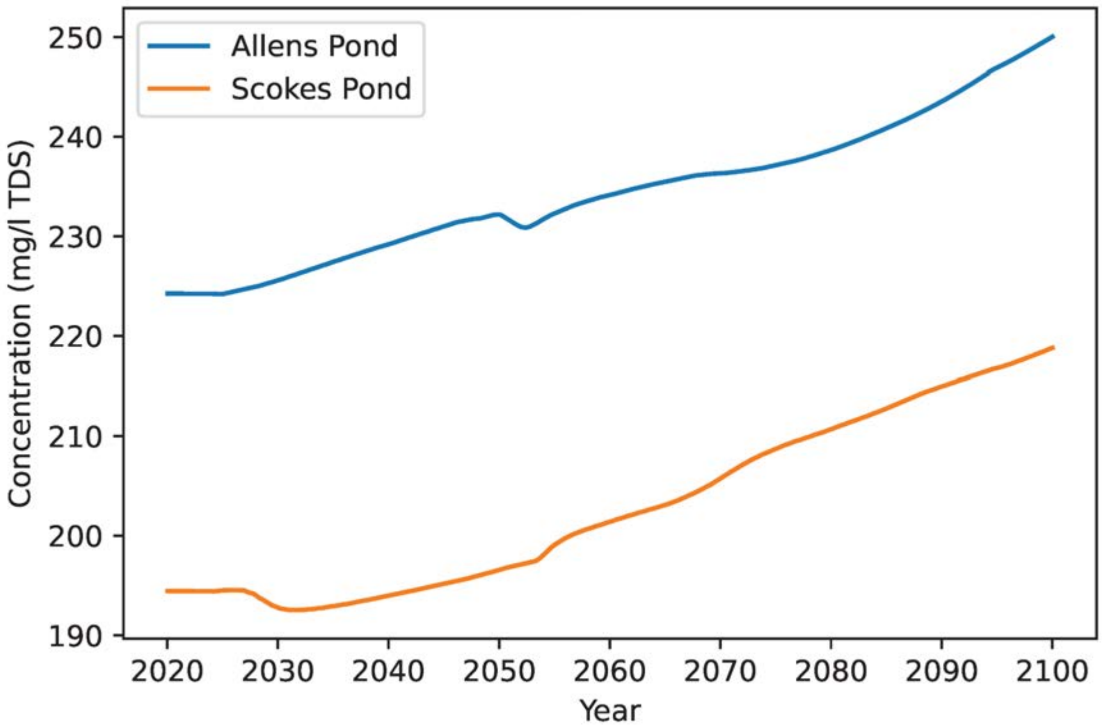

Figure 9.2.5-1: Simulated TDS concentrations of Allens Pond and Scokes Pond from 2020 to 2100 for Simulation 2. See Figure 9.1.3-2 for locations of these ponds.

Task 9.2.6 Assess likelihood of Impacts of changes in the terrestrial freshwater recharge on saline intrusion

Total dissolved solid concentrations at year 2100 increase by 0 to 15,476 mg/l when reducing terrestrial recharge by 15% (2100 Simulation 4 TDS minus 2100 Simulation 1 TDS) (Figure 9.2.6-2). The 1,000-10,000 mg/l Δ TDS zone generally ranges from 100 to 200 m wide at the water table, but can increase to ~700 m wide in coastal marsh and estuary environments in the northern region of the model. Salinity increases from reduced recharge occur because terrestrial hydraulic heads decrease with less recharge, so the hydraulic gradient between the saltwater and freshwater decreases allowing more saline water to flow landward.

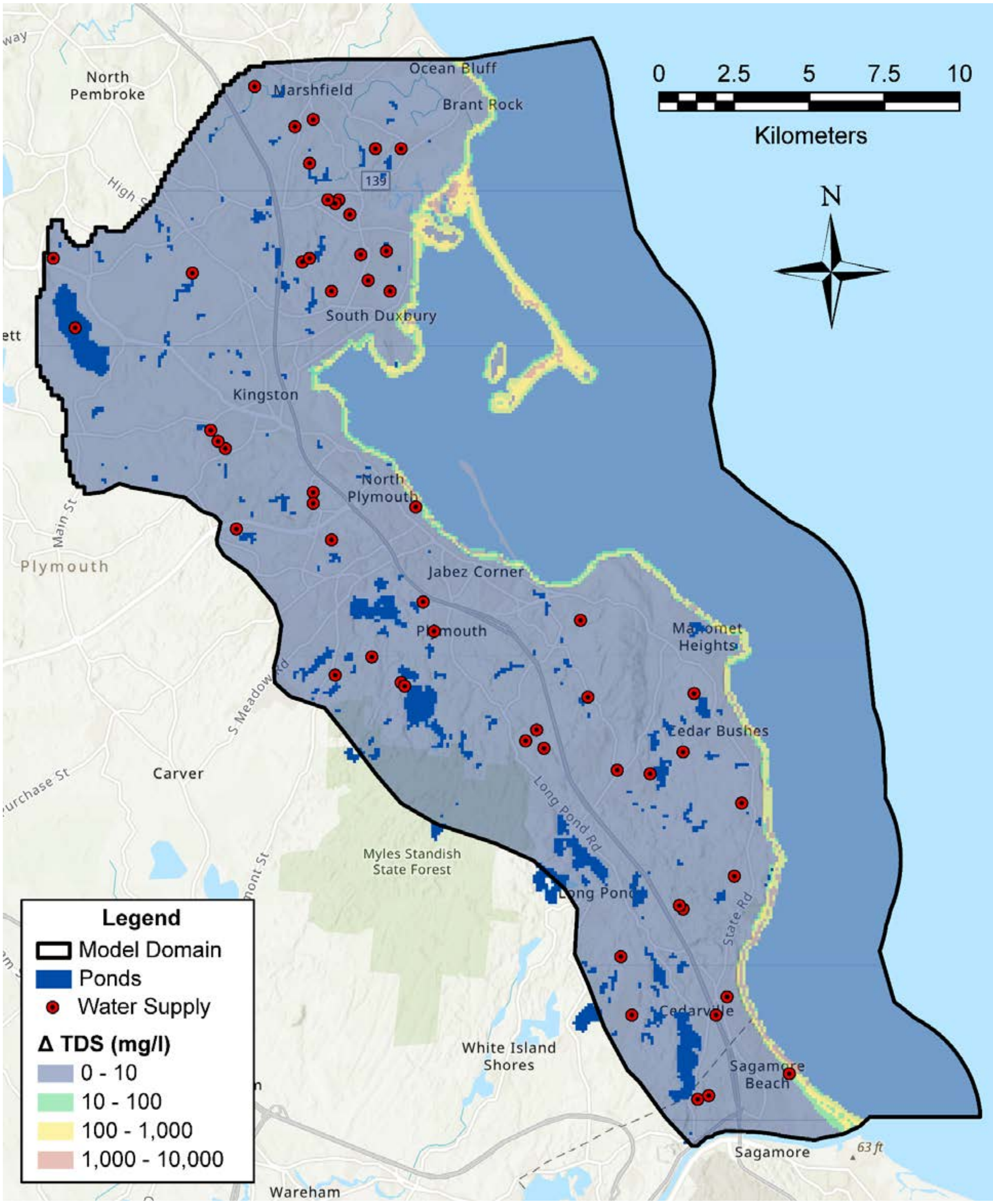

Figure 9.2.6-1: Concentration difference at year 2100 (Δ TDS) between Simulations 1 and 4 showing landward migration of the interface mixing zone from 15% reduction in terrestrial recharge.

Task 9.3 Recommendations For Short and Long term Solutions to Remedy Possible Impacts of Saltwater Intrusion

The forward looking modeling presented above shows limited onshore migration (~200 meters) of the freshwater-saltwater interface. These scenarios looked at the migration due to subsurface migration of saltwater alone. These simulations do not account for storm surge, tidal processes and other surface water inundation processes. The movement of coastal surface waters into freshwater ponds and streams is an additional important process to introduce saltwater into the shallow near surface aquifer. Future studies should investigate surface water inundation into sensitive surface water features. There are existing efforts regionally to model impacts such as these including grounds at the Woodwell Climate center and the University of Massachusetts-Lowell. Therefore, monitoring of surface water salinity in key locations throughout the town is critical. Additionally we are proposing several locations for subsurface salinity measurements to take place throughout the model domain and the town of plymouth.

Based on the modeling results presented we have the following recommendations and suggestions:

- Encourage the town of Plymouth to develop a data dashboard to post salinity observations of town water supplies wells on an annual basis.
- Raise funds to perform an airborne electromagnetic geophysical survey of coastal areas to image the extent of saltwater intrusion (to test modeling) and document the hydrostratigraphic architecture of key coastal areas (See section 9.1.4)
- Develop an early warning system for subsurface salinity changes in key coastal areas (documented in Task 9.3.1)
- Develop and maintain a salinity database for surface and groundwaters across the town.
- Consider the suggested recommendations in section 9.3.2 for optimal placement of freshwater production wells.

Actions to continue to control salinity intrusion into aquifer:

- Continue to re-infiltrate wastewater into the onshore aquifer system.
- Reduce overall freshwater pumping and encourage water-use reductions.
- Limit the extent of saltwater intrusion into surface water bodies - as this represents quick pathways for subsurface infiltration of saltwater into aquifer

Task 9.3.1 Determine optimal placement of early warning system for saline intrusion

Figure 9.3.1-1 shows the suggested locations for an early warning system for salinity monitoring due to sea-level rise. The wells should be nested piezometers (3 in total) screened at different depths throughout the aquifer. Wells should be geophysically logged and completed using a professional hydrogeologist consultancy. Real-time pressure and salinity monitoring should be installed in the wells and maintained quarterly. These are also areas that could be subject to overwash events and would be helpful for monitoring impacts of storms on near surface aquifer salinity.

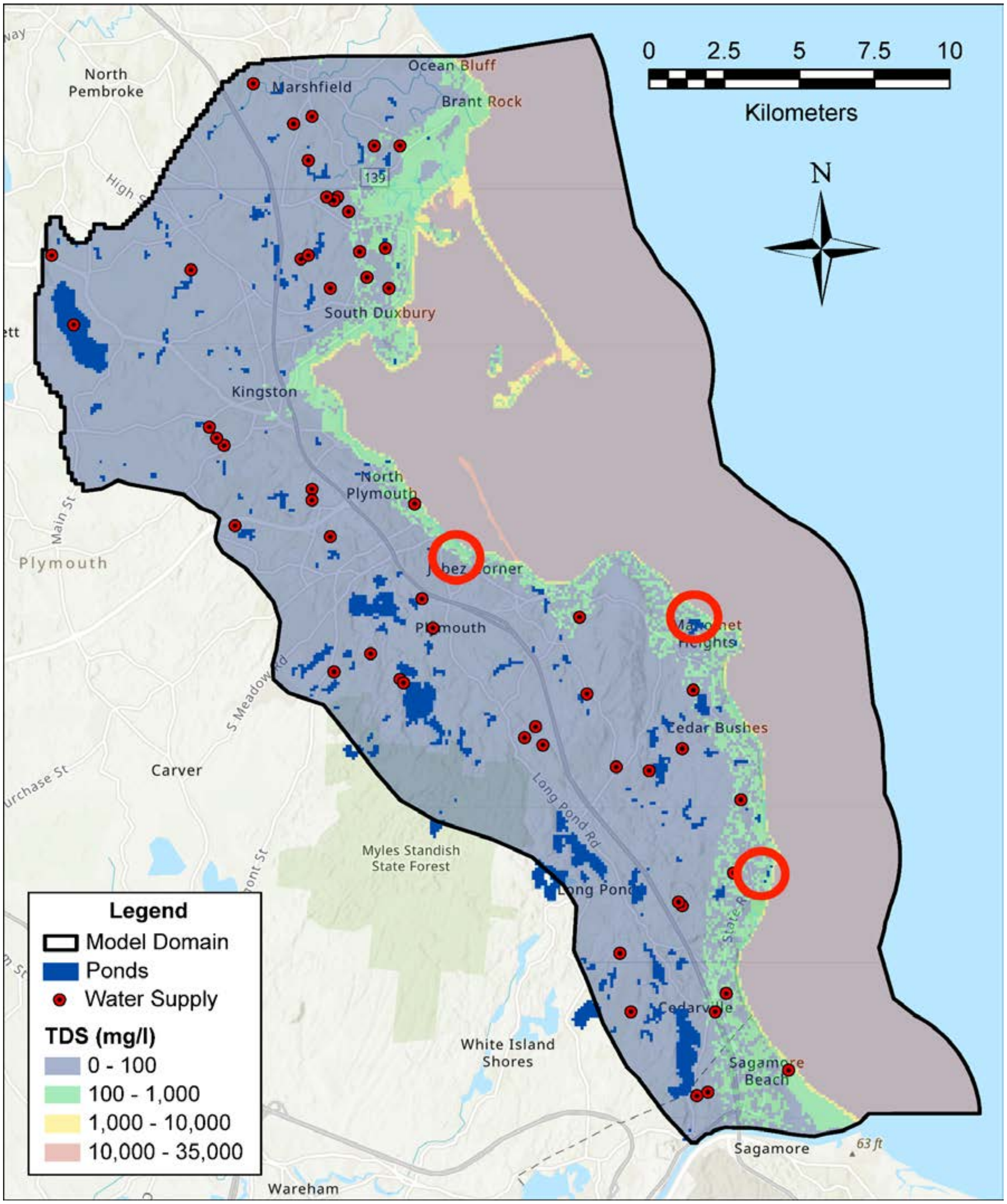

Figure 9.3.1-1: Map showing pond locations, water supply wells, and simulated total dissolved solids in relation to suggested locations (red circles) for salinity monitoring wells.

Task 9.3.2 Determine optimal location for replacement or new freshwater production wells

Figure 9.3.2-1 shows the current production well sites and capture zones for the region. We also show the simulated salinity zones of the aquifer. While the siting of wells is a complex process that involves land use, aquifer considerations, and logistical details - we suggest that moving new public water supplies in the region outside of the green contours associated with TDS between 100-1,000 mg/l.

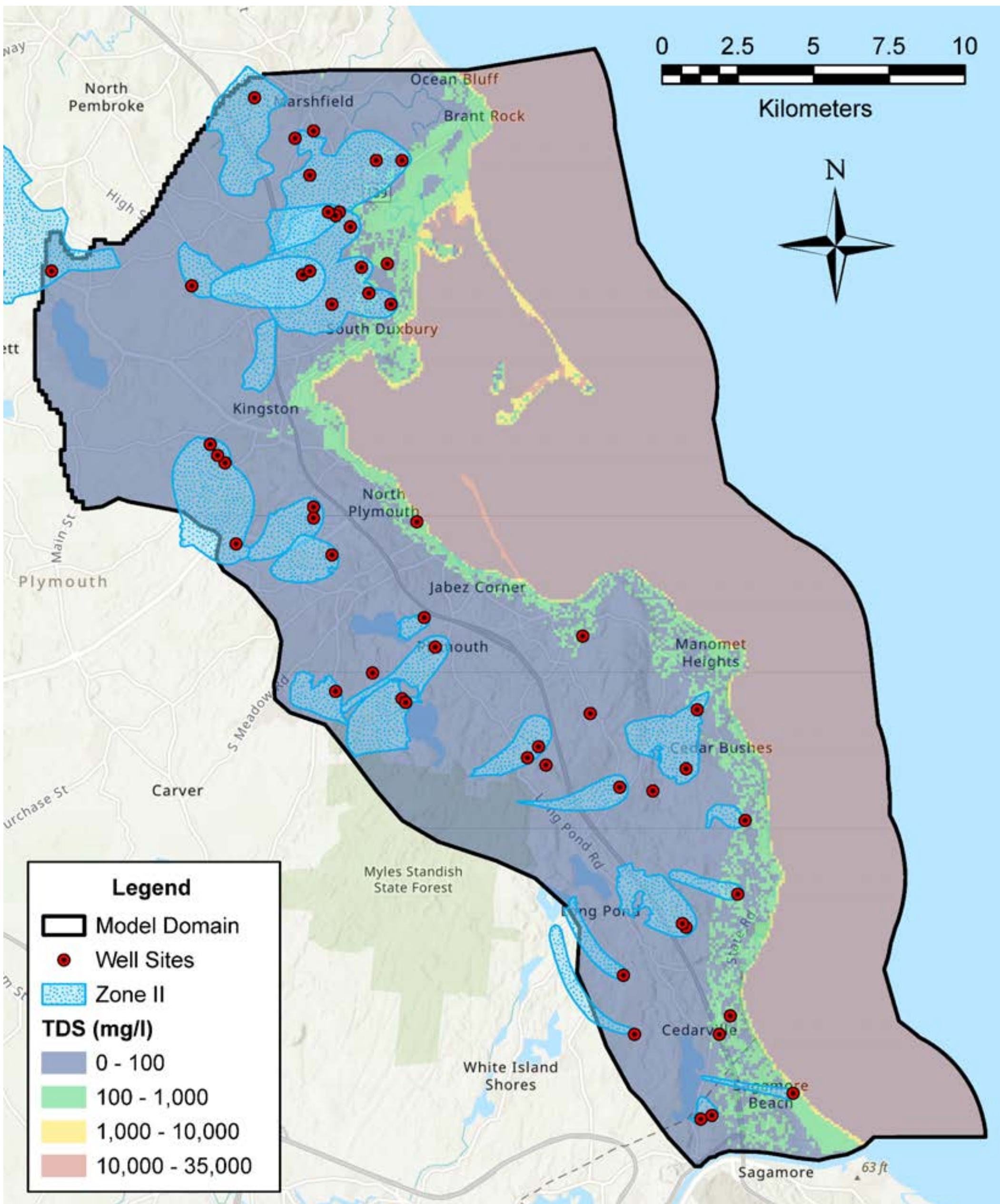

Figure 9.3.2-1: Map showing pond locations, water supply wells, and simulated total dissolved solids in relation to suggested criteria for locating new water supply development wells.

References

Andrews, B.D., Baldwin, W.E., Sampson, D.W., and Schwab, W.C., 2018, Continuous bathymetry and elevation models of the Massachusetts coastal zone and continental shelf (ver. 3.0, December 2019): U.S. Geological Survey data release, https://doi.org/10.5066/F72806T7.

Douglas, E. and Kirshen, P., 2022, Climate Change Impacts and Projections for the Greater Boston Area.

Goebel, M., Knight, R., & Halkjær, M., 2019, Mapping saltwater intrusion with an airborne electromagnetic method in the offshore coastal environment, Monterey Bay, California. Journal of Hydrology: Regional Studies, 23, 100602.

Hansen, B.P. and Lapham, W.W., 1992, Geohydrology and simulated ground water flow, Plymouth-Carver aquifer, southeastern Massachusetts: Water-resources investigations report 90-4204.

Langevin, C.D., Hughes, J.D., Provost, A.M., Russcher, M.J., Niswonger, R.G., Panday, Sorab, Merrick, Damian, Morway, E.D., Reno, M.J., Bonelli, W.P., and Banta, E.R., 2023, MODFLOW 6 Modular Hydrologic Model version 6.4.2: U.S. Geological Survey Software Release, 28 June 2023, https://doi.org/10.5066/P9FL1JCC.

Mabee, S.B., W.P. Clement, C. Duncan, M. Pope, K. Moynahan, R. Miller, H. Davis and A. Low, 2022, A data set of depth to bedrock described in drill holes and geophysical surveys for Massachusetts - Release 1. Massachusetts Geological Survey Data Release DR22-01. Spreadsheet, metadata and 15-page report.

Masterson, J.P., Carlson, C.S., and Walter, D.A., 2009, Hydrogeology and simulation of groundwater flow in the Plymouth-Carver-Kingston-Duxbury aquifer system, southeastern Massachusetts: U.S. Geological Survey Scientific Investigations Report 2009–5063, 110 p.

Stone, B.D., and Stone, J.R., 2019, Geologic Origins of Cape Cod, Massachusetts; Guidebook for the Northeast Friends of the Pleistocene, 82nd Annual Fieldtrip, May 31-June 2, 2019: Massachusetts Geological Survey Open-file Report 19-01, 63 p.